Dynamic Analysis of the Conditional Oscillator Underlying Slow Waves in Thalamocortical Neurons

François David, Vincenzo Crunelli, Nathalie Leresche, Régis C Lambert

Dynamic Analysis of the Conditional Oscillator Underlying Slow Waves in Thalamocortical Neurons

François David [1, 2, 3, 4, 5, 6, 7]*, Vincenzo Crunelli [1, 8], Nathalie Leresche [5, 6, 7] and Régis C. Lambert [5, 6, 7]*

[1] Neuroscience Division, School of Biosciences, Cardiff University, Cardiff, UK, [2] Lyon Neuroscience Research Center, Centre National de la Recherche Scientifique UMR 5292, Lyon, France, [3] Lyon Neuroscience Research Center, Institut National de la Santé et de la Recherche Médicale U1028, Lyon, France, [4] Faculté de Médecine, Université Claude Bernard, Lyon, France, [5] Sorbonne Universités, UPMC Université Paris 06, UM 119, Neuroscience Paris Seine, Paris, France, [6] Centre National de la Recherche Scientifique, UMR 8246, Neuroscience Paris Seine, Paris, France, [7] Institut National de la Santé et de la Recherche Médicale, U1130, Neuroscience Paris Seine, Paris, France, [8] Department of Physiology and Biochemistry, University of Malta, Msida, Malta

During non-REM sleep the EEG shows characteristics waves that are generated by the dynamic interactions between cortical and thalamic oscillators. In thalamic neurons, low-threshold T-type Ca^{2+} channels play a pivotal role in almost every type of neuronal oscillations, including slow (<1 Hz) waves, sleep spindles and delta waves. The transient opening of T channels gives rise to the low threshold spikes (LTSs), and associated high frequency bursts of action potentials, that are characteristically present during sleep spindles and delta waves, whereas the persistent opening of a small fraction of T channels, (i.e., $I_{Twindow}$) is responsible for the membrane potential bistability underlying sleep slow oscillations. Surprisingly thalamocortical (TC) neurons express a very high density of T channels that largely exceed the amount required to generate LTSs and therefore, to support certain, if not all, sleep oscillations. Here, to clarify the relationship between T current density and sleep oscillations, we systematically investigated the impact of the T conductance level on the intrinsic rhythmic activities generated in TC neurons, combining *in vitro* experiments and TC neuron simulation. Using bifurcation analysis, we provide insights into the dynamical processes taking place at the transition between slow and delta oscillations. Our results show that although stable delta oscillations can be evoked with minimal T conductance, the full range of slow oscillation patterns, including groups of delta oscillations separated by *Up* states ("grouped-delta slow waves") requires a high density of T channels. Moreover, high levels of T conductance ensure the robustness of different types of slow oscillations.

Keywords: thalamus, sleep slow wave, delta waves, T-type calcium channels, bifurcation, computational modeling

INTRODUCTION

Sleep is characterized by the regular appearance of stereotyped sequences of EEG waves (Achermann and Borbely, 1997; Steriade, 2006; Crunelli et al., 2014) that are generated by the dynamic interaction between, and require the integrity of both cortical and thalamic oscillators (Steriade et al., 1993b; Crunelli and Hughes, 2010; David et al., 2013; Lemieux et al., 2014). The various cellular activities that are expressed by thalamocortical (TC) neurons during sleep

oscillations tightly depend on the expression of low-threshold T-type Ca^{2+} channels (T channels; Leresche et al., 1991; Williams et al., 1997a; Crunelli et al., 2014). In fact, while these channels are almost fully inactivated in the range of membrane potentials associated to the wake state (but see Lambert et al., 2014), during non-REM sleep the progressive reduction in the depolarizing tone exerted by modulatory afferents onto both cortical and thalamic neurons (McCormick, 1992) allows T channel de-inactivation. As a consequence, the recruitment of de-inactivated T channels generates large inward currents resulting in transient depolarizations, called low-threshold spike (LTS). Thus, rhythmic LTSs, often crowned by bursts of high-frequency (>200 Hz) action potentials, are present in TC neurons during sleep spindles (7–14 Hz; Steriade et al., 1993b; Contreras and Steriade, 1996; David et al., 2013) and delta waves (0.5–4 Hz; Steriade et al., 1993a), and an LTS is almost invariably present at the start of each *Up* state of sleep slow oscillations in TC neurons (**Figure 2A**; Steriade et al., 1993a). *Up* states interspersed with periods of hyperpolarization (i.e., *Down* states) are the thalamic cellular hallmarks of sleep slow (<1 Hz) waves (**Figure 2A**). Moreover, slow waves group together periods of sleep spindle and delta waves (Steriade, 2006), and these periods of delta oscillations that are visible during the *Down* state of the cellular counterpart of sleep slow waves in TC neurons have been named "grouped-delta slow waves" (**Figure 2A**; Steriade et al., 1993a; Hughes et al., 2002; Crunelli et al., 2015). Importantly, the interaction of the leak current with a small number of de-inactivated T channels opening with a low (but non-zero) probability in a narrow range of membrane potentials around −60 mV (i.e., $I_{Twindow}$; Perez-Reyes, 2003; Dreyfus et al., 2010) is necessary for the generation of the membrane potential bistability that in TC neuron underlies the expression of the *Up* and *Down* state dynamics of sleep slow waves (Williams et al., 1997a; Toth et al., 1998; Hughes et al., 2002; Dreyfus et al., 2010).

Despite these key roles for T channels in sleep waves, it is still not known how the density of the T-type Ca^{2+} current (I_T) affects each sleep oscillation. We previously demonstrated that robust LTSs can be evoked even when up to 70% of the T channel population is pharmacologically blocked (Dreyfus et al., 2010), suggesting that the high T channel expression that is present in TC neurons is not required for LTS generation during delta and slow oscillations. A high T channel expression in TC neurons, however, may be crucial to provide a level of $I_{Twindow}$ sufficient for the generation of the *UP* and *Down* state dynamics underlying slow oscillations in this type of thalamic neurons.

Here, using both *in vitro* experiments and TC neuron simulation, we systematically investigated the impact of the T conductance level on the various sleep oscillations intrinsically generated in TC neurons. Since I_T can be controlled by various modulatory mechanisms (Lambert et al., 2006; Huc et al., 2009), we also investigated the effects of the ATP- and voltage-dependent regulation that potentiates the amplitude of I_T in sensory TC neurons (Leresche et al., 2004). Our results show that although stable delta oscillations can be evoked with minimal T conductance, the full range of slow oscillation patterns, including simple *Up* and *Down* state transitions and the more complex "grouped-delta slow waves," requires a high density of T channels

or a potentiation of the current. Moreover, high levels of I_T ensure the robustness of different slow wave oscillations over a larger range of leak conductance values.

MATERIALS AND METHODS

Slice Preparation and Recordings

All procedures involving experimental animals were carried out in accordance with the UK Animals (Scientific Procedure) Act, 1986 and Cardiff Ethical Review Committee guidelines. Thalamic slices from a 3-year old cat were prepared as described previously (Hughes et al., 2002). Briefly, the cat was deeply anesthetized with a mixture of O2 and NO2(2:1) and 5% isoflurane, a wide craniotomy was performed to remove the brain and coronal slices of the thalamus (300–400 μm) that contain the dorsal lateral geniculate nucleus (LGN), were prepared and incubated at 35°C for 1 h before being maintained at room temperature. For recording, slices were perfused with a warmed (35 ± 1°C) continuously oxygenated (95% O₂, 5% CO₂) artificial CSF (ACSF) containing the following (in mM): 134 NaCl, 2 KCl, 1.25 KH_2PO_4, 1 $MgSO_4$, 2 $CaCl_2$, 16 $NaHCO_3$, and 10 glucose.

Intracellular recordings, using the current clamp technique, were performed with standard-wall glass microelectrodes filled with 1 M potassium acetate (resistance, 80–120 MOhm) and connected to an Axoclamp-2A amplifier (Molecular Devices, Sunnyvale, CA) operating in bridge mode. Membrane potentials were digitized at 25 kHz using pClamp 9 (Molecular Devices). All recordings in the LGN were obtained from lamina A. Impaled cells were identified as TC neurons using established criteria (Pirchio et al., 1997; Turner et al., 1997). Sleep oscillations (including slow oscillations <1 Hz) were induced by bath application of 50 μM (±)-1-aminocyclopentane-*trans*-1,3-dicarboxylic acid (*trans*-ACPD) followed by changes in steady-state current injections to allow neurons to express different slow oscillations, as previously shown (Hughes et al., 2004). SR95531 (gabazine, 10 μM), CGP54626 (20 μM), D-APV (50 μM), and CNQX (10 μM) were included in the bath solution to block both GABA-A and GABA-B as well as NMDA and AMPA glutamatergic synaptic inputs onto TC neurons, respectively. The T channel antagonist, TTA-P2 (kindly provided by Merck Inc, USA), was made up as a 10 mM stock solution in dimethylsulfoxide and kept at −20°C until use at a final concentration of 500 nM.

Simulations

All simulations were performed using the Matlab based programs (Mathworks, Natick, MA) or xppaut continuation application developed by Ermentrout (2002), and were run with a fixed time step of 0.02 ms using the Euler integration method. For simulations, the system was initiated at a point close to the *Up* state and the simulation results were analyzed only after stabilization of the simulation result (i.e., 50 s after the start of the simulation).

The single-compartment TC neuron model based on (Williams et al., 1997a; Hughes et al., 2002), expressed the essential physiological properties of these neurons (**Figure 2**).

Ionic currents were simulated following Hodgkin-Huxley formalism.

The membrane potential (V) was described by the following equation:

$$C_m dV/dt = -I_{Leak} - I_T - I_{TP} - I_h - I_{CAN} - I_{Na} - I_{Kir},$$

where Cm (50 pF) is the membrane capacitance, I_{Leak} is a potassium leak current (reversal potential = -95 mV), I_T is the T current, I_{TP} is the potentiated component of the T current, I_h is the hyperpolarization-activated nonspecific cationic current, I_{CAN} is the Ca^{2+} activated non-selective cation current, I_{Na} is the voltage-dependent Na^+ current and I_{Kir} is K^+ current which includes the inward and delayed rectifier components. All current units are pA. Each current was simulated as follows:

I_T:

$$I_T = g_T \cdot m^3(V) \cdot h(V) \cdot (V(t) - E_T),$$

where g_T is the maximal conductance and $E_T = 180$ mV is the reversal potential for Ca^{2+} flux. m and h are activation and inactivation variables, respectively, which are defined as follows:

$$m_{\infty,T} = \frac{1}{1 + \exp\left(-\frac{v+63}{7.8}\right)},$$

$$\tau_{m,T} = 0.612 + \frac{1}{\exp\left(\frac{V+16.8}{18.2}\right) + exp\left(-\frac{V+131.6}{16.7}\right)}$$

$$h_{\infty,T} = \frac{1}{1 + \exp\left(\frac{v+83.5}{6.3}\right)},$$

if V < -80 $\tau_{h,T} = \exp\left(\frac{V+467}{66.6}\right)$

otherwise $\tau_{h,T} = \left[28 + \exp\left(\frac{V+21.88}{10.2}\right)\right]$

I_{TP}:

The potentiated component of the T current was modeled by multiplying the T current by a voltage-dependent coefficient P representing the fraction of phosphorylated ("potentiated") channels (see Leresche et al., 2004 for details)

$$I_{TP} = g_{TP} \cdot m^3(V) \cdot h(V) \cdot P(V) \cdot (V(t) - E_T)$$

The voltage dependence of P is related to the steady-state inactivation of I_T as followed (**Figure 1A**):

$$P_{\infty,T} = 1 - h_{\infty,T} \quad \tau_{P,T} = 3000 - \frac{2700}{(1 + \exp(-(V + 65)))}$$

I_h:

$$I_h = g_h \cdot m^3(V) \cdot (V(t) - E_h)$$

gh = 8 nS

$$m_{\infty,h} = \frac{1}{1 + \exp(\frac{v+75}{5.5})}, \text{ if V} < -77.57,$$

$$\tau_h = \frac{120819.5}{\exp(-0.0614 \cdot V)} \text{ otherwise } \tau_h = \frac{29.54}{\exp(0.0458 \cdot V)}$$
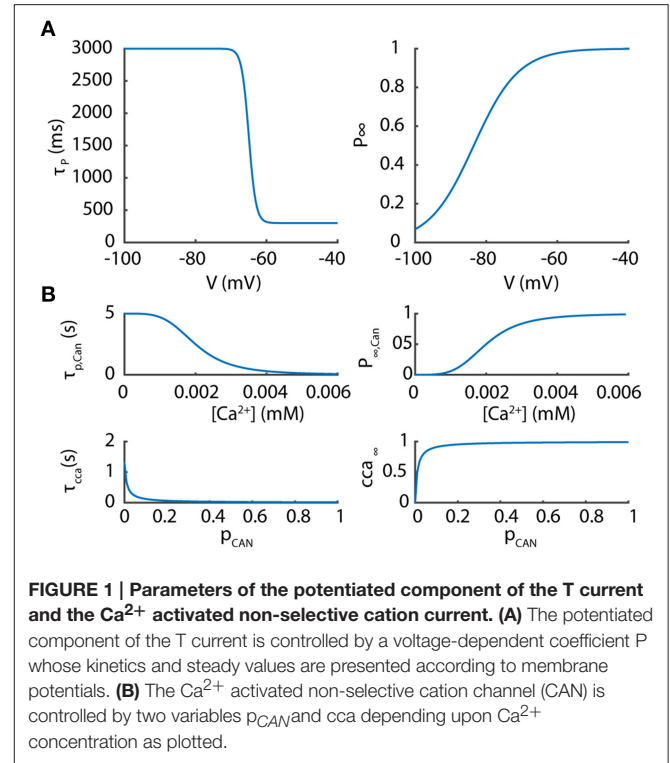
FIGURE 1 | Parameters of the potentiated component of the T current and the Ca^{2+} activated non-selective cation current. (A) The potentiated component of the T current is controlled by a voltage-dependent coefficient P whose kinetics and steady values are presented according to membrane potentials. (B) The Ca^{2+} activated non-selective cation channel (CAN) is controlled by two variables p_{CAN} and cca depending upon Ca^{2+} concentration as plotted.

I_{CAN} (**Figure 1B**):

$$I_{CAN} = g_{CAN} \cdot cca \cdot (V(t) - E_{CAN})$$

$g_{CAN} = 12$ nS

$$cca_{\infty,CAN} = \frac{a_{cca}}{a_{cca} + b_{cca}} \quad \tau_{cca,CAN} = \frac{1}{a_{cca} + b_{cca}}$$

$$a_{cca} = 0.075 \cdot p_{CAN} \quad b_{cca} = 0.00075$$

$$p_{\infty,CAN} = \frac{1.25 \cdot 10^7 \cdot [Ca2+]^4}{1.25 \cdot 10^7 \cdot [Ca2+]^4 + 0.2} \quad \tau_{p,CAN} = \frac{1}{1.25 \cdot 10^7 \cdot [Ca2+]^4 + 0.2}$$

The calcium concentration ($[Ca^{2+}]$, in mM) is governed by the Ca^{2+} influx through T channels and a Ca^{2+} pump that controls intracellular Ca^{2+} levels.

$$\left[Ca^{2+}\right] = -(I_T + I_{TP})\frac{0.0052}{Area \cdot Depth} - 5 \cdot \left[Ca^{2+}\right]$$

where Area is 5000 μm^2 and Depth is 0.1 μm.

I_{Na}:

$$I_{Na} = g_{Na}m(V)^3 \cdot h(V) \cdot (V - E_{Na+})$$

$$g_{Na} = 1320 nS$$

$$a_{m,Na} = 0.32 \frac{-V - 49.3}{(e^{(-V-49.3)/4} - 1)}$$

$$b_{m,Na} = 0.28 \frac{-V - 22.3}{1 - e^{(-V-22.3)/5}}$$

$$m_{\infty,Na} = \frac{a_{m,Na}}{a_{m,Na} + b_{m,Na}} \quad \tau_{m,Na} = \frac{1}{a_{m,Na} + b_{m,Na}}$$

$$a_{h,Na} = 0.128 \, e^{\frac{-V-45.4}{18}} \quad b_{h,Na} = \frac{4}{e^{\frac{-V-22.4}{5}}+1}$$

$$h_{\infty,Na} = \frac{a_{h,Na}}{a_{h,Na}+b_{h,Na}} \quad \tau_{h,Na} = \frac{1}{a_{h,Na}+b_{h,Na}}$$

I_{Kir}:

$$I_{Kir} = g_K \cdot n^4(V) \cdot (V - E_K)$$

$$g_K = 600nS$$

$$a_{n,K} = 9.93 \cdot 0.016 \cdot \frac{-V-57.2+35.1/9.93}{(e^{(-V-57.2+35.1/9.93)/5}-1)}$$

$$b_{n,K} = 0.25 \cdot 9.93 \cdot e^{\frac{-V-57.2+20/9.93}{40}}$$

$$n_{\infty,K} = \frac{a_{n,K}}{a_{n,K}+b_{n,K}} \quad \tau_{n,K} = \frac{1}{a_{n,K}+b_{n,K}}$$

Data Analysis

Numerical integrations of the equations without g_{Na} were performed with the software package XXPAUT (Ermentrout, 2002) to compute the periodic and steady-state solutions as a function of a given parameter (either g_{Leak} or g_T). The orbits (or periodic solutions) were detected by continuation of the equation system i.e., by computing the equilibrium solutions of the differential equations of the membrane potential and of other variables by the forward and backward temporal integration of these equations starting from the bifurcation fixed points with Xppaut (http://www.math.pitt.edu/~bard/xpp/xpp.html). The bifurcation parameter (g_{Leak}) was varied on adaptative step size between 0.0001 and 0.1 nS and a discretization interval number for periodic orbit of 50. g_{Na} was not used on a first approximation as this fast component easily prevents the system from converging to a stable orbit solution on a slow temporal scale. Stable solutions found without g_{Na} were nonetheless confirmed or infirmed in the system that included g_{Na} in the following steps of the analysis. For *Up* and *Down* state detection, the membrane potential was down-sampled at 1 kHz. *Up* states were defined as the proportion of simulated time where the membrane potential was > -65 mV. An *Up* state episode during slow oscillation was defined as a finite temporal continuous sequence during which the membrane potential remained > -65 mV for more than 500 ms. A *Down* state during slow oscillation was defined as a continuous temporal sequence where the membrane potential remained below the -65 mV threshold. The average membrane potential during an *Up* state was estimated by averaging all membrane potential values belonging to the *Up* state. The number of LTSs per slow oscillation was estimated as the number of *Down* states (which always precede a LTS) divided by the number of *Up* states. Slow oscillation frequency was estimated by averaging instantaneous frequencies measured for each slow oscillation cycle that was defined as starting and finishing with the LTS that is invariably present at the start of each *Up* state.
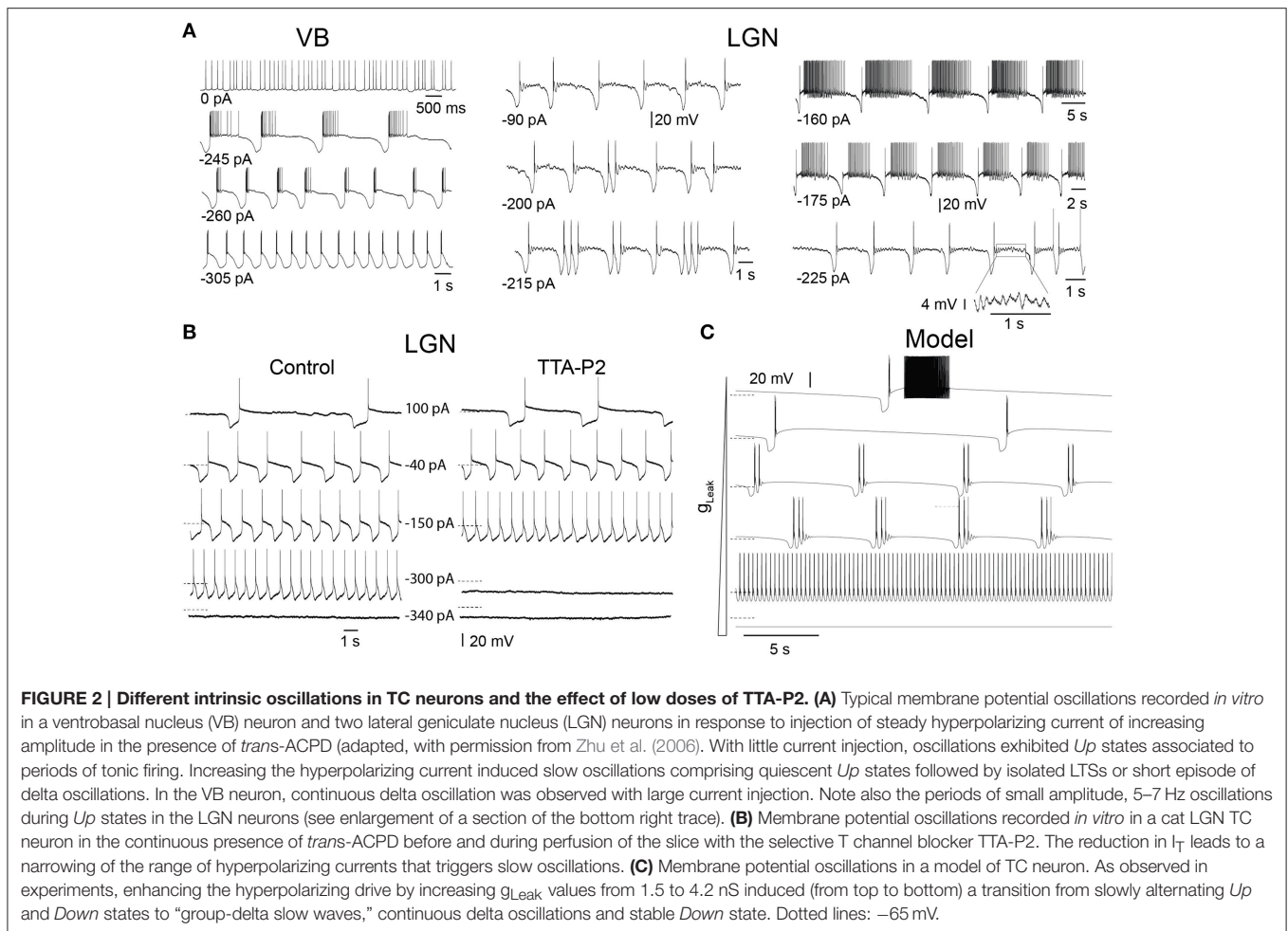
RESULTS

In slices, TC neurons of sensory (lateral and medial geniculate, VB), motor (ventrolateral), and intralaminar (centrolateral)

thalamic nuclei recorded in the presence of *trans*-ACPD exhibit stereotypical firing patterns and oscillations when submitted to steady hyperpolarizing currents of increasing amplitudes, as we previously described (Hughes et al., 2002; Zhu et al., 2006; Crunelli et al., 2012, 2014): from stable *UP* states, at times showing tonic firing, to slow *Up* and *Down* state oscillations, "grouped-delta slow waves" (i.e., slow oscillations with delta oscillations during the *DOWN* state), pure delta oscillations (1–4 Hz) and stable silent *DOWN* states (**Figure 2A**). These activities result from the interplay of intrinsic TC neuron conductances, including the T-type Ca^{2+} current (I_T), with both its transient and window ($I_{Twindow}$) components, the hyperpolarization activated Na^+-K^+ current (I_h), the Ca^{2+} activated non-selective cation current (I_{CAN}), the inward rectifying potassium current (I_{Kir}) and the leak K^+ current (I_{leak}) (Williams et al., 1997b; Hughes et al., 2002). In order to investigate how I_T density affects the expression of these various oscillations, we compared in LGN TC neurons the range of injected steady hyperpolarizing current required to observe the distinct patterns of oscillations in control conditions and when I_T was partially blocked by the selective antagonist TTA-P2 (Dreyfus et al., 2010). As shown in **Figure 2B**, the range of steady hyperpolarizing currents where slow oscillations could occur under control condition (355 ± 31 pA, $n = 5$) was clearly smaller in the presence of TTA-P2 (198 ± 28 pA, $n = 5$), indicating that a reduction in I_T drastically weakens the generation of the slow oscillation.

To thoroughly analyze the relationship between the T conductance and the ability of TC neuron to generate various sleep-related oscillations, we constructed a minimal single compartment model of a TC neuron that, upon g_{Leak} variation, satisfactorily reproduced the activities observed *in vitro* in response to different steady hyperpolarizing currents (**Figure 2C**). Although not strictly equivalent, we chose to vary g_{Leak} instead of simulating a hyperpolarizing current injection in order to mimic the natural changes observed across various sleep stages. Using the bifurcation analysis of this dynamic system (without I_{Na} to facilitate analysis, see Materials and Methods), we first calculated the extent of stable *Up* and *Down* states as a function of g_T and g_{Leak}. As shown in **Figure 3A**, increasing g_T favors a stable *Up* state and larger g_{Leak} values are required to switch the system to a stable *DOWN* state. As already mentioned, $I_{Twindow}$ contributes to the resting membrane potential around -60mV (Dreyfus et al., 2010). Since departure from the stable *Up* state occurs around this potential, a stronger I_{Leak} is required to counteract the depolarizing drive resulting from a large g_T and a consequently greater $I_{Twindow}$. The graph also shows the presence of a region of membrane potential instability (delineated by the green and yellow dashed lines in **Figure 3A**) which occurs for a range of g_{Leak} and g_T values. This area of instability can be associated to particular oscillatory dynamics: slow oscillations and continuous delta oscillations (**Figure 3B**). As already observed experimentally (see Figure 9 in Soltesz and Crunelli, 1992), for some g_T values where the system has a subcritical Hopf bifurcation point (Wang and Rinzel, 2002; Amarillo et al., 2015), oscillatory regimes and a stable *Down* state can theoretically occur in the same g_{Leak} domain.
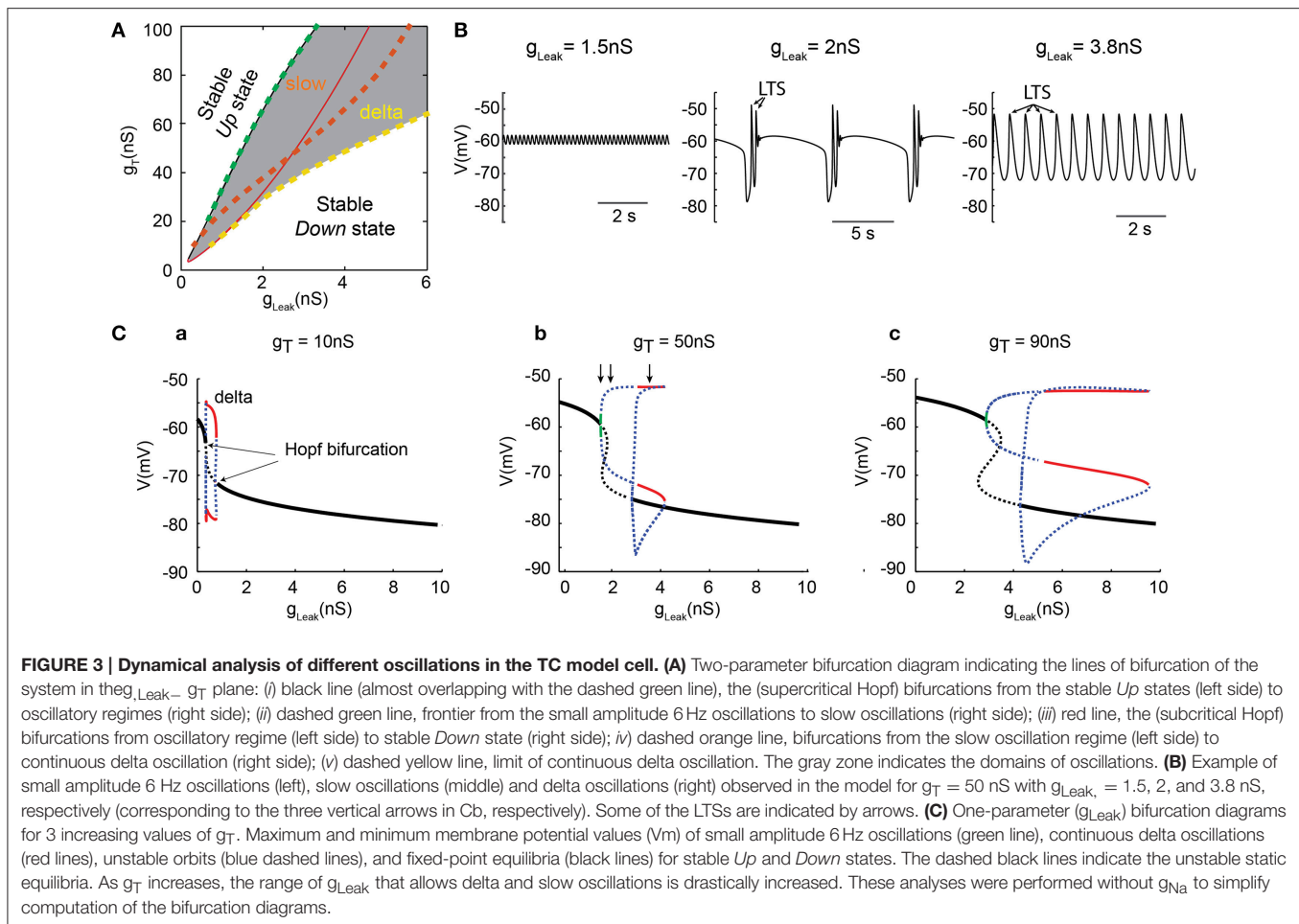
For a small g_T (**Figure 3Ca**), the one-dimension bifurcation diagram of the model system as a function of g_{Leak} remains simple

FIGURE 2 | Different intrinsic oscillations in TC neurons and the effect of low doses of TTA-P2. (A) Typical membrane potential oscillations recorded *in vitro* in a ventrobasal nucleus (VB) neuron and two lateral geniculate nucleus (LGN) neurons in response to injection of steady hyperpolarizing current of increasing amplitude in the presence of *trans*-ACPD (adapted, with permission from Zhu et al. (2006). With little current injection, oscillations exhibited *Up* states associated to periods of tonic firing. Increasing the hyperpolarizing current induced slow oscillations comprising quiescent *Up* states followed by isolated LTSs or short episode of delta oscillations. In the VB neuron, continuous delta oscillation was observed with large current injection. Note also the periods of small amplitude, 5–7 Hz oscillations during *Up* states in the LGN neurons (see enlargement of a section of the bottom right trace). **(B)** Membrane potential oscillations recorded *in vitro* in a cat LGN TC neuron in the continuous presence of *trans*-ACPD before and during perfusion of the slice with the selective T channel blocker TTA-P2. The reduction in I_T leads to a narrowing of the range of hyperpolarizing currents that triggers slow oscillations. **(C)** Membrane potential oscillations in a model of TC neuron. As observed in experiments, enhancing the hyperpolarizing drive by increasing g_{Leak} values from 1.5 to 4.2 nS induced (from top to bottom) a transition from slowly alternating *Up* and *Down* states to "group-delta slow waves," continuous delta oscillations and stable *Down* state. Dotted lines: −65 mV.

with departure from the stable *Up* or *Down* states involving Hopf bifurcations. The stable periodic orbits correspond to pure delta oscillations (red lines in **Figure 3Ca**) that do not overlap with the regions where stable *Up* or *Down* states exist. This indicates that small g_T values allow only 3 robust exclusive activity patterns in TC neurons: stable *Up* state, pure delta oscillations and stable *Down* state. However, when g_T is increased, the bifurcation diagram becomes more complex (**Figures 3Cb,c**). At departure from the stable *Up*-state, small periodic orbits involving membrane potential oscillations of a few millivolts in amplitude (**Figure 3B** left) at 6 Hz (or higher frequency) are present for a very narrow range of g_{Leak} (green line in **Figures 3Cb,c**). Such low-amplitude oscillations that occur close to −60 mV are consistently present in our simulations. Although these oscillations cannot be easily related to any physiologically defined membrane potential waveform of TC neurons, they resemble oscillations that occasionally appear in the *Up* state of slow oscillations in these neurons (**Figure 2A**; see Hughes et al., 2002; Zhu et al., 2006), and have been suggested to represent the intrinsic dynamic contribution of TC neurons to synaptically generated spindle oscillations (Wang, 1994). As g_{Leak} further increases, unstable orbit cycles (blue dots in **Figures 3Cb,c**), corresponding to the complex "grouped-delta

slow waves" (**Figure 3B** middle), occur for a large range of g_{Leak} before the stable periodic orbits corresponding to pure delta oscillations (**Figure 3B** right) could develop (red lines in **Figures 3Cb,c**). Therefore, although delta oscillations are already present with small g_T values, only a larger g_T allows the occurrence of the full dynamics observed in TC neurons, including "grouped-delta slow waves."

In order to more precisely describe the different slow wave patterns present for a given g_T value, simulations were then run while systematically varying g_T and g_{Leak} (in the presence of g_{Na}; **Figure 4**). Confirming the conclusions of the bifurcation diagrams, analysis of the membrane potential dynamics as a function of g_{Leak} indicates that only delta oscillations occur for the smallest g_T value (10 nS, **Figures 4B,C**). When g_T is increased, in addition to continuous delta oscillations, slow oscillations with *Up* states that always start with a LTS are observed in a narrow range of g_{Leak} (**Figures 4A–C**). For larger values of g_T, "grouped-delta slow waves" are present and this firing pattern can be observed in a large range of g_{Leak} values that expands as g_T increases (**Figures 4A–C**). Further quantification of the slow oscillation parameters indicates that for g_T values associated with a robust slow oscillation pattern ($g_T \geq 30$ nS), the ranges of *Up*-state duration and slow wave frequencies remain

FIGURE 3 | Dynamical analysis of different oscillations in the TC model cell. (A) Two-parameter bifurcation diagram indicating the lines of bifurcation of the system in the g_{Leak}– g_T plane: (*i*) black line (almost overlapping with the dashed green line), the (supercritical Hopf) bifurcations from the stable *Up* states (left side) to oscillatory regimes (right side); (*ii*) dashed green line, frontier from the small amplitude 6 Hz oscillations to slow oscillations (right side); (*iii*) red line, the (subcritical Hopf) bifurcations from oscillatory regime (left side) to stable *Down* state (right side); *iv*) dashed orange line, bifurcations from the slow oscillation regime (left side) to continuous delta oscillation (right side); (*v*) dashed yellow line, limit of continuous delta oscillation. The gray zone indicates the domains of oscillations. **(B)** Example of small amplitude 6 Hz oscillations (left), slow oscillations (middle) and delta oscillations (right) observed in the model for $g_T = 50$ nS with $g_{Leak,} = 1.5$, 2, and 3.8 nS, respectively (corresponding to the three vertical arrows in Cb, respectively). Some of the LTSs are indicated by arrows. **(C)** One-parameter (g_{Leak}) bifurcation diagrams for 3 increasing values of g_T. Maximum and minimum membrane potential values (Vm) of small amplitude 6 Hz oscillations (green line), continuous delta oscillations (red lines), unstable orbits (blue dashed lines), and fixed-point equilibria (black lines) for stable *Up* and *Down* states. The dashed black lines indicate the unstable static equilibria. As g_T increases, the range of g_{Leak} that allows delta and slow oscillations is drastically increased. These analyses were performed without g_{Na} to simplify computation of the bifurcation diagrams.
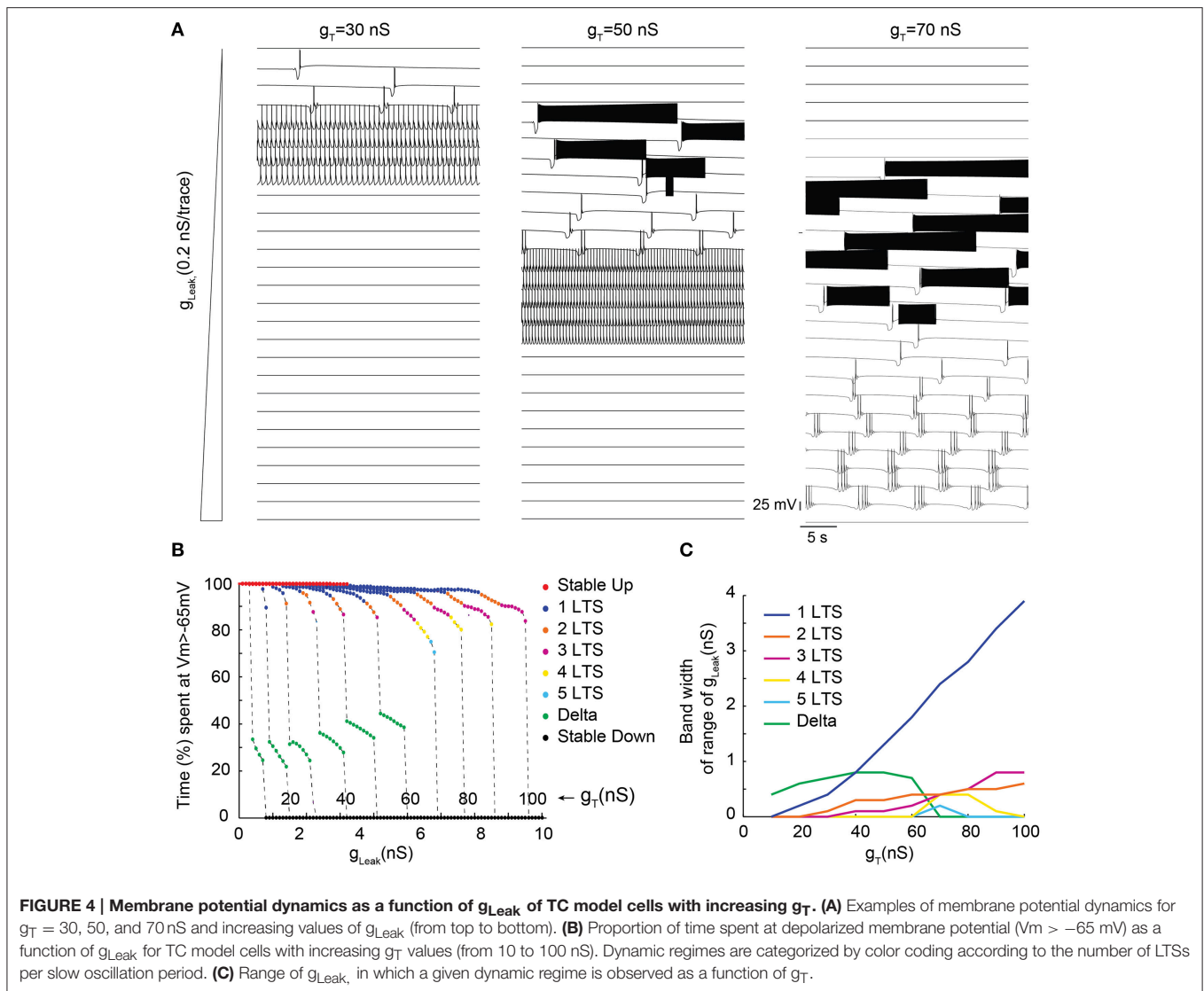
stable (**Figures 5A,B**), but the maximal value of the *Up* state membrane potential increases proportionally to g_T (**Figure 5C**). These increasingly more depolarized *Up* states may result from both a stronger $I_{Twindow}$ directly linked to the larger g_T and the consequently stronger I_{CAN} due to the larger Ca^{2+} entry occurring during the T channel activation that generates the LTS at the beginning of each *Up* state.

Surprisingly, for the highest g_T values (>70 nS), although long sequences of "grouped-delta slow waves" are present (**Figure 4C**), our model cell did not anymore display continuous delta oscillations but abruptly switched from "grouped-delta slow waves" to stable *Down* states when g_{Leak} increased. While the bifurcation diagrams previously calculated for large g_T values (**Figures 3A,Cc**) predicted an increase of the range of g_{Leak} values where stable periodic delta orbits corresponding to continuous delta oscillations may develop, stable *Down* states were the only solutions observed in our simulations (**Figure 4C**). Such dominance of the stable *Down* state over continuous delta oscillations was due to the presence of action potentials on top of the LTS which elicit large high K^+ rectifying currents. Indeed, in simulations performed without g_{Na} continuous delta oscillations were observed for some g_{Leak} values (data not shown).

Although the prominent I_T in TC neurons mainly results from a high channel expression, we previously demonstrated

that in neurons of sensory thalamic nuclei, I_T amplitude is also transiently potentiated by a phosphorylation (ATP-dependent) mechanism, which exclusively occurs when the channels are inactivated, i.e., it increases with membrane depolarization (Leresche et al., 2004). To study how this additional mechanism that drastically controls the T current amplitude in this population of TC neurons contributes to their firing dynamics a new set of simulations was run where part of the total I_T was due to a "potentiated" T conductance (g_{TP}). The kinetics, amplitude and voltage-dependence of this g_{TP} mimic the effect and properties of the described phosphorylation mechanism (see Materials and Methods for further details; Leresche et al., 2004). When I_T was increased by introducing g_{TP} in the model, a strengthening of the slow oscillation which occurred in a larger range of g_{Leak} values is once again observed (**Figure 6C**; also compare **Figures 6A,B** with **Figures 4A,B**). However, for a given value of T conductance, negligible differences in the bifurcation diagrams are observed when comparing the dynamical behaviors supported either by non-potentiated currents or by a combination of non-potentiated and potentiated currents (**Figures 6D–G**). Hence, the peculiar biophysical properties of the potentiated T conductance do not significantly modify the membrane potential dynamics of slow oscillations. Nevertheless a close examination of the oscillatory

FIGURE 4 | Membrane potential dynamics as a function of g_{Leak} of TC model cells with increasing g_T. (A) Examples of membrane potential dynamics for g_T = 30, 50, and 70 nS and increasing values of g_{Leak} (from top to bottom). **(B)** Proportion of time spent at depolarized membrane potential (Vm > −65 mV) as a function of g_{Leak} for TC model cells with increasing g_T values (from 10 to 100 nS). Dynamic regimes are categorized by color coding according to the number of LTSs per slow oscillation period. **(C)** Range of g_{Leak}, in which a given dynamic regime is observed as a function of g_T.

regimes shows that for T conductance values where both "grouped-delta slow waves" and continuous delta developed (**Figure 6B**, g_T 60 nS), the continuous delta disappeared upon introduction of the voltage-dependent potentiation (**Figure 6B**, g_T 30 nS+g_{TP} 30 nS). This suggests that compared to a simple increase in g_T, this ATP-dependent T channel regulation can selectively enhance the occurrence of slow oscillations of TC neurons at the expenses of delta oscillations.
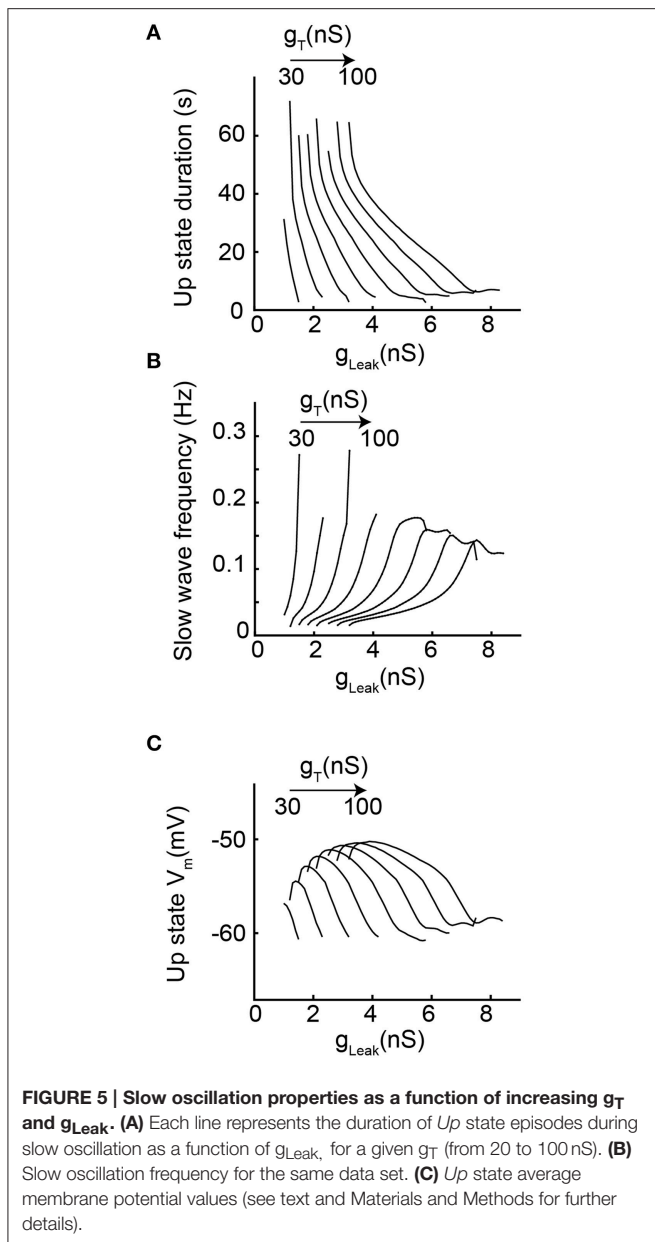
DISCUSSION

Since their first development (Rose and Hindmarsh, 1989), TC neuron models have gained in precision and completeness (Destexhe et al., 1998), thus allowing detailed analysis of the dynamical processes that are intrinsic to these neurons (Destexhe and Sejnowski, 2003; Amarillo et al., 2015). Our current model adds to this knowledge by providing for the first time insights into the dynamical processes that take place at the transition

between slow and delta oscillations. In particular, our results strongly suggest that the high g_T of TC neurons, either due to channel expression or regulation, is not required to generate full-blown LTSs during delta and slow oscillations but is necessary for the generation of the *Up* and *Down* state dynamics underlying the slow oscillation of these neurons (David et al., 2013; Crunelli et al., 2014).

Contrary to the interpretation of the original *in vitro* and *in vivo* studies (see Crunelli et al., 2015), it is now well established that the full expression of slow oscillations requires both cortical and thalamic activities. In particular, combining ensemble recordings of single TC neurons and reverse microdialysis, we recently showed that slow wave frequency is strongly reduced following intrathalamic application of either TTX or TTA-P2 in both anesthetized and naturally sleeping rats (David et al., 2013). In agreement with these data, mice with a Cav3.1 deletion in the thalamus (but not in the cortex) experience frequent arousals during sleep (Anderson et al., 2005), supporting the importance of thalamic T channels in stabilizing sleep rhythms. Moreover,

FIGURE 5 | Slow oscillation properties as a function of increasing g_T and g_{Leak}. (A) Each line represents the duration of *Up* state episodes during slow oscillation as a function of g_{Leak}, for a given g_T (from 20 to 100 nS). **(B)** Slow oscillation frequency for the same data set. **(C)** *Up* state average membrane potential values (see text and Materials and Methods for further details).

the biophysical mechanisms underlying the conditional thalamic oscillator responsible in TC neurons for the full manifestation of different types of slow oscillation depends on the membrane potential bistability that is created by the interaction between $I_{Twindow}$ and I_{Leak} (Williams et al., 1997a; Toth et al., 1998; Crunelli et al., 2006). TC neurons present a small $I_{Twindow}$ (a few tens of pA; Dreyfus et al., 2010) and any decrease in this current may drastically impact its ability to play a significant physiological role. Our simulations results indicate that the high T channel expression in TC neurons is crucial to generate a large enough $I_{Twindow}$ capable of supporting the *Up* and *Down* states dynamics of slow oscillations over a large range of g_{Leak} values. This was clearly confirmed by our *in vitro* recordings showing that partial block of the I_T by TTA-P2 drastically reduces

the range of steady hyperpolarizing currents that can generate intrinsic slow oscillations in TC neurons.

In addition, our simulations have indicated that a large g_T is also essential for the appearance of "grouped-delta slow waves." As indicated above, during slow waves the voltage-dependence of $I_{Twindow}$ creates the membrane potential bistability but the rhythmic occurrence of *Up* and *Down* states relies on the dynamics of I_{CAN} (Hughes et al., 2002). Indeed, upon Ca^{2+} entry via the T channels these mixed cationic channels generates a transient depolarizing current that adds to $I_{Twindow}$ to set the membrane potential of the *Up* state. As intracellular Ca^{2+} slowly return to its basal level, the progressive decrease of I_{CAN} reduces this membrane potential up to the point where the stable *Up* state equilibrium disappears and the membrane potential switches to the *Down*-state. With medium g_T values, Ca^{2+} entry during LTS is moderate and I_{CAN} activation, together with $I_{Twindow}$, is not strong enough to counteract a strong I_{Leak} and thus to generate the stable equilibrium necessary for an *Up*-state. Consequently, TC neurons go into continuous delta oscillations. However, with higher g_T values, Ca^{2+} accumulation after a few delta oscillation cycles is sufficient to maximally activate I_{CAN} and thus set an *Up* state equilibrium that terminates a delta oscillation episode.

Importantly, when our simulations included g_{Na} we did not observe continuous delta oscillations for high or potentiated T channel conductances. Indeed, during natural sleep, thalamic delta oscillations appear to occur mostly in discrete groups during the down state of slow oscillations in both TC and nucleus reticularis thalami neurons (Steriade et al., 1993c; Timofeev and Steriade, 1996) and there is no evidence supporting the presence of continuous delta oscillations in TC neurons *in vivo*. Therefore, one can hypothesize that as suggested in **Figure 3A** strong T channel expression may prevent the appearance of continuous intrinsic rhythmicity at delta frequency in TC neurons. Interestingly, we previously showed that the maximal amplitude of I_T is highly variable across neurons of different thalamic nuclei and even in different TC neurons within a nucleus (Leresche et al., 2004). Therefore, further modeling studies should aim to investigate how this heterogeneity in T channel density among TC neurons interacts with other intrinsic conductance expression such as I_{CAN} or Ih to impact oscillatory dynamics.

Finally, one has to consider that the slow oscillation modeled here is generated intrinsically by single TC neurons (i.e., recorded in the presence of both glutamate and GABA blockers) and thus without the influence of either excitatory cortical and inhibitory inputs. Although this should represent the basic cellular mechanism explaining the conditional role played by the thalamus in sleep slow waves generation (Crunelli and Hughes, 2010), the precise interactions between this intrinsic mechanism and the complex thalamocortical activities (Sheroziya and Timofeev, 2014) remain to be clarified. Along the same line our simulations cannot inform on the firing dynamics of TC neurons during the expression of absence seizures since this abnormal activity requires the integrity of the thalamocortical network (Crunelli and Leresche, 2002). However the present results may help to better understand firing patterns observed during general anesthesia where the EEG mostly includes spindle and delta waves (Franks, 2008). In particular, phase 2 of the
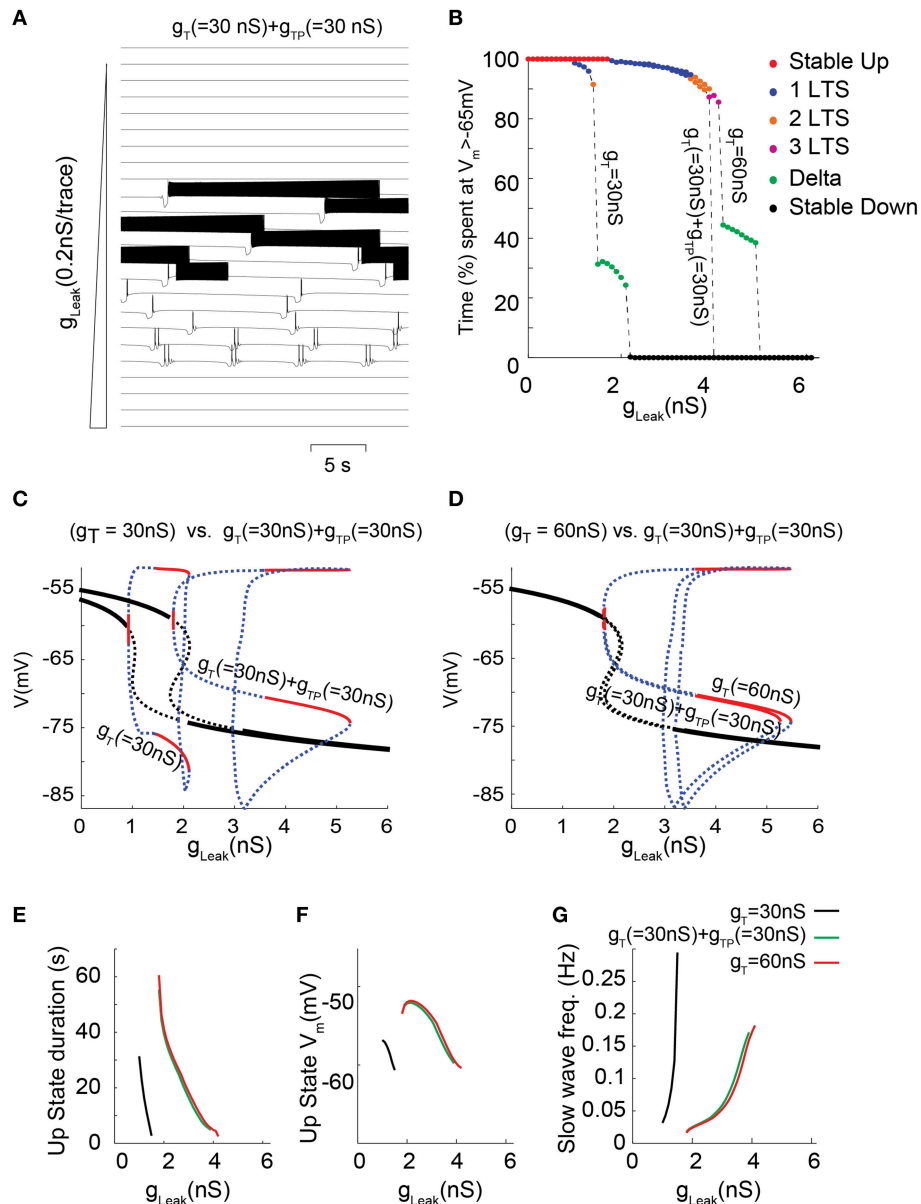
FIGURE 6 | Membrane potential dynamics as a function of g_{Leak} for a TC model cell that incorporates I_T potentiation. (A) Typical example of membrane potential dynamics for $g_T = 30$ nS $+ g_{TP} = 30$ nS for increasing g_{Leak}, values. **(B)** Proportion of time spent at depolarized membrane potential (Vm > −65 mV) as a function of g_{Leak} for TC model cells with $g_T = 30$ nS; $g_T = 30$ nS $+ g_{TP} = 30$ nS; and $g_T = 60$ nS (same color code as in **Figure 4B** to indicate dynamical regimes). **(C,D)** Effect on the one-parameter (g_{Leak} on x-axis) bifurcation diagrams of either adding a potentiated T conductance (C, $g_T = 30$ nS vs. $g_T = 30$ nS $+ g_{TP} = 30$ nS) or replacing half of the T conductance by a potentiated T conductance (D, $g_T = 60$ nS vs. $g_T = 30$ nS $+ g_{TP} = 30$ nS). Same legend as in **Figure 3C**. **(E–G)** Slow oscillation characteristics observed in model TC cells with either $g_T = 30$ nS (black); $g_T = 30$ nS $+ g_{TP} = 30$ nS (green) or $g_T = 60$ nS (red). **(E)** Each line represents the duration of *Up* state episodes during slow oscillation as a function of g_{Leak}, for a given g_T and g_{TP}. **(F)** Slow oscillation frequency for the same data set. **(G)** *Up* state average membrane potential values.

maintenance period is characterized by an increase in delta (0–4 Hz) activity (Brown et al., 2010). At clinically relevant concentrations, a number of volatile general anesthetics have been shown to inhibit both recombinant and native T channels (Orestes and Todorovic, 2010; Eckle et al., 2012), a result which was considered at first glance in contradiction with the occurrence of delta oscillations. However, (Eckle et al., 2012)

showed that anesthetic doses of isoflurane only inhibits 20 to 60% of I_T but induce a marked decrease of $I_{Twindow}$ in TC neurons. In this respect, our simulations clearly indicate that such partial inhibition of I_T should indeed favor the occurrence of continuous delta oscillations, at least in TC neurons. In agreement with this view, a partial block of I_T by *in vivo* administration of TTA-related compounds also produce sedative

effects in behaving mice (Uebele et al., 2009; Kraus et al., 2010), further illustrating the complex relationship between the amount of g_T and various sleep-related activities.

AUTHOR CONTRIBUTIONS

FD, VC, NL, RL contribute to the design of the work, the acquisition, analysis and interpretation of data. FD, VC, NL, RL contribute to the manuscript and approve the final version.

REFERENCES

Achermann, P., and Borbely, A. A. (1997). Low-frequency (< 1 Hz) oscillations in the human sleep electroencephalogram. *Neuroscience* 81, 213–222.

Amarillo, Y., Mato, G., and Nadal, M. S. (2015). Analysis of the role of the low threshold currents IT and Ih in intrinsic delta oscillations of thalamocortical neurons. *Front. Comput. Neurosci.* 9:52. doi: 10.3389/fncom.2015.00052

Anderson, M. P., Mochizuki, T., Xie, J., Fischler, W., Manger, J. P., Talley, E. M., et al. (2005). Thalamic Cav3.1 T-type Ca2+ channel plays a crucial role in stabilizing sleep. *Proc. Natl. Acad. Sci. U.S.A.* 102, 1743–1748. doi: 10.1073/pnas.0409644102

Brown, E. N., Lydic, R., and Schiff, N. D. (2010). General anesthesia, sleep, and coma. *N. Engl. J. Med.* 363, 2638–2650. doi: 10.1056/NEJMra0808281

Contreras, D., and Steriade, M. (1996). Spindle oscillation in cats: the role of corticothalamic feedback in a thalamically generated rhythm. [published erratum appears in J Physiol (Lond) 1996 Mar 15;491(Pt 3):889]. *J. Physiol. (Lond).* 490, 159–179.

Crunelli, V., Cope, D. W., and Hughes, S. W. (2006). Thalamic T-type Ca2+ channels and NREM sleep. *Cell Calcium* 40, 175–190. doi: 10.1016/j.ceca.2006.04.022

Crunelli, V., David, F., Leresche, N., and Lambert, R. C. (2014). Role for T-type Ca2+ channels in sleep waves. *Pflugers Archiv.* 466, 735–745. doi: 10.1007/s00424-014-1477-3

Crunelli, V., David, F., Lorincz, M. L., and Hughes, S. W. (2015). The thalamocortical network as a single slow wave-generating unit. *Curr. Opin. Neurobiol.* 31, 72–80. doi: 10.1016/j.conb.2014.09.001

Crunelli, V., and Hughes, S. W. (2010). The slow (<1 Hz) rhythm of non-REM sleep: a dialogue between three cardinal oscillators. *Nat. Neurosci.* 13, 9–17. doi: 10.1038/nn.2445

Crunelli, V., and Leresche, N. (2002). Childhood absence epilepsy: genes, channels, neurons and networks. *Nat. Rev. Neurosci.* 3, 371–382. doi: 10.1038/nrn811

Crunelli, V., Lorincz, M., and Hughes, S. W. (2012). Activity of cortical and thalamic neurons during the slow (<1Hz) oscillation in the mouse *in vivo*. *Pflugers Arch.* 463, 73–88. doi: 10.1007/s00424-011-1011-9

David, F., Schmiedt, J. T., Taylor, H. L., Orban, G., Di Giovanni, G., Uebele, V. N., et al. (2013). Essential thalamic contribution to slow waves of natural sleep. *J. Neurosci.* 33, 19599–19610. doi: 10.1523/JNEUROSCI.3169-13.2013

Destexhe, A., Neubig, M., Ulrich, D., and Huguenard, J. (1998). Dendritic low-threshold calcium currents in thalamic relay cells. *J. Neurosci.* 18, 3574–3588.

Destexhe, A., and Sejnowski, T. J. (2003). Interactions between membrane conductances underlying thalamocortical slow-wave oscillations. *Physiol. Rev.* 83, 1401–1453. doi: 10.1152/physrev.00012.2003

Dreyfus, F. M., Tscherter, A., Errington, A. C., Renger, J. J., Shin, H. S., Uebele, V. N., et al. (2010). Selective T-type calcium channel block in thalamic neurons reveals channel redundancy and physiological impact of I(T)window. *J. Neurosci.* 30, 99–109. doi: 10.1523/JNEUROSCI.4305-09.2010

Eckle, V. S., Digruccio, M. R., Uebele, V. N., Renger, J. J., and Todorovic, S. M. (2012). Inhibition of T-type calcium current in rat thalamocortical neurons by isoflurane. *Neuropharmacology* 63, 266–273. doi: 10.1016/j.neuropharm.2012.03.018

Ermentrout, B. (2002). *Simulating, Analyzing and Animating Dynamical Systems: A Guide to Xppaut for Researchers and Student.* 1st Edn. Philadelphia, PA: Society for Industrial and Applied Mathematics.

Franks, N. P. (2008). General anaesthesia: from molecular targets to neuronal pathways of sleep and arousal. *Nat. Rev. Neurosci.* 9, 370–386. doi: 10.1038/nrn2372

Huc, S., Monteil, A., Bidaud, I., Barbara, G., Chemin, J., and Lory, P. (2009). Regulation of T-type calcium channels: signalling pathways and functional implications. *Biochim. Biophys. Acta* 1793, 947–952. doi: 10.1016/j.bbamcr.2008.11.003

Hughes, S. W., Cope, D. W., Blethyn, K. L., and Crunelli, V. (2002). Cellular mechanisms of the slow (1 Hz) oscillation in thalamocortical neurons *in vitro*. *Neuron* 33, 947–958. doi: 10.1016/S0896-6273(02)00623-2

Hughes, S. W., Lorincz, M., Cope, D. W., Blethyn, K. L., Kekesi, K. A., Parri, H. R., et al. (2004). Synchronized oscillations at alpha and theta frequencies in the lateral geniculate nucleus. *Neuron* 42, 253–268. doi: 10.1016/S0896-6273(04)00191-6

Kraus, R. L., Li, Y., Gregan, Y., Gotter, A. L., Uebele, V. N., Fox, S. V., et al. (2010). *In vitro* characterization of T-type calcium channel antagonist TTA-A2 and in vivo effects on arousal in mice. *J. Pharmacol. Exp. Ther.* 335, 409–417. doi: 10.1124/jpet.110.171058

Lambert, R. C., Bessaih, T., Crunelli, V., and Leresche, N. (2014). The many faces of T-type calcium channels. *Pflugers Archiv.* 466, 415–423. doi: 10.1007/s00424-013-1353-6

Lambert, R. C., Bessaih, T., and Leresche, N. (2006). Modulation of neuronal T-type calcium channels. *CNS Neurol. Disord. Drug Targets* 5, 611–627. doi: 10.2174/187152706779025544

Lemieux, M., Chen, J. Y., Lonjers, P., Bazhenov, M., and Timofeev, I. (2014). The impact of cortical deafferentation on the neocortical slow oscillation. *J. Neurosci.* 34, 5689–5703. doi: 10.1523/JNEUROSCI.1156-13.2014

Leresche, N., Hering, J., and Lambert, R. C. (2004). Paradoxical potentiation of neuronal T-type Ca2+ current by ATP at resting membrane potential. *J. Neurosci.* 24, 5592–5602. doi: 10.1523/JNEUROSCI.1038-04.2004

Leresche, N., Lightowler, S., Soltesz, I., Jassik-Gerschenfeld, D., and Crunelli, V. (1991). Low-frequency oscillatory activities intrinsic to rat and cat thalamocortical cells. *J Physiol (Lond)* 441, 155–174.

McCormick, D. A. (1992). Neurotransmitter actions in the thalamus and cerebral cortex and their role in neuromodulation of thalamocortical activity. *Prog. Neurobiol.* 39, 337–388.

Orestes, P., and Todorovic, S. M. (2010). Are neuronal voltage-gated calcium channels valid cellular targets for general anesthetics? *Channels* 4, 518–522. doi: 10.4161/chan.4.6.12873

Perez-Reyes, E. (2003). Molecular physiology of low-voltage-activated t-type calcium channels. *Physiol. Rev.* 83, 117–161. doi: 10.1152/physrev.00018.2002

Pirchio, M., Turner, J. P., Williams, S. R., Asprodini, E., and Crunelli, V. (1997). Postnatal development of membrane properties and delta oscillations in thalamocortical neurons of the cat dorsal lateral geniculate nucleus. *J. Neurosci.* 17, 5428–5444.

Rose, R. M., and Hindmarsh, J. L. (1989). The assembly of ionic currents in a thalamic neuron. I. The three-dimensional model. Proceedings of the Royal Society of London. *Ser. B Biol. Sci.* 237, 267–288.

Sheroziya, M., and Timofeev, I. (2014). Global intracellular slow-wave dynamics of the thalamocortical system. *J. Neurosci.* 34, 8875–8893. doi: 10.1523/JNEUROSCI.4460-13.2014

Soltesz, I., and Crunelli, V. (1992). A role for low-frequency, rhythmic synaptic potentials in the synchronization of cat thalamocortical cells. *J. Physiol. (Lond).* 457, 257–276.

Steriade, M. (2006). Grouping of brain rhythms in corticothalamic systems. *Neuroscience* 137, 1087–1106. doi: 10.1016/j.neuroscience.2005.10.029

Steriade, M., Contreras, D., Curro Dossi, R., and Nunez, A. (1993a). The slow (< 1 Hz) oscillation in reticular thalamic and thalamocortical neurons: scenario of sleep rhythm generation in interacting thalamic and neocortical networks. *J. Neurosci.* 13, 3284–3299.

Steriade, M., McCormick, D. A., and Sejnowski, T. J. (1993b). Thalamocortical oscillations in the sleeping and aroused brain. *Science* 262, 679–685.

Steriade, M., Nunez, A., and Amzica, F. (1993c). Intracellular analysis of relations between the slow (< 1 Hz) neocortical oscillation and other sleep rhythms of the electroencephalogram. *J. Neurosci.* 13, 3266–3283.

Timofeev, I., and Steriade, M. (1996). Low-frequency rhythms in the thalamus of intact-cortex and decorticated cats. *J. Neurophysiol.* 76, 4152–4168.

Toth, T. I., Hughes, S. W., and Crunelli, V. (1998). Analysis and biophysical interpretation of bistable behaviour in thalamocortical neurons [In Process Citation]. *Neuroscience* 87, 519–523.

Turner, J. P., Anderson, C. M., Williams, S. R., and Crunelli, V. (1997). Morphology and membrane properties of neurones in the cat ventrobasal thalamus *in vitro*. *J. Physiol. (Lond).* 505, 707–726.

Uebele, V. N., Nuss, C. E., Fox, S. V., Garson, S. L., Cristescu, R., Doran, S. M., et al. (2009). Positive allosteric interaction of structurally diverse T-type calcium channel antagonists. *Cell Biochem. Biophys.* 55, 81–93. doi: 10.1007/s12013-009-9057-4

Wang, X. J. (1994). Multiple dynamical modes of thalamic relay neurons: rhythmic bursting and intermittent phase-locking. *Neuroscience* 59, 21–31.

Wang, X. J., and Rinzel, J. (2002). *The Handbook of Brain Theory and Neural Networks.* Cambridge, MA: The MIT Press.

Williams, S. R., Toth, T. I., Turner, J. P., Hughes, S. W., and Crunelli, V. (1997a). The 'window' component of the low threshold Ca2+ current produces input signal amplification and bistability in cat and rat thalamocortical neurones. *J. Physiol. (Lond).* 505, 689–705.

Williams, S. R., Turner, J. P., Hughes, S. W., and Crunelli, V. (1997b). On the nature of anomalous rectification in thalamocortical neurones of the cat ventrobasal thalamus *in vitro*. *J. Physiol. (Lond).* 505, 727–747.

Zhu, L., Blethyn, K. L., Cope, D. W., Tsomaia, V., Crunelli, V., and Hughes, S. W. (2006). Nucleus- and species-specific properties of the slow (<1 Hz) sleep oscillation in thalamocortical neurons. *Neuroscience* 141, 621–636. doi: 10.1016/j.neuroscience.2006.04.069